

# Characterization of Nanostructural ZnSe Prepared by Inert Gas Condensation Method

I. K. El-Zawawi and A. M. El-Shabiny

Solid State Physics Department., National Research Center,  
Dokki, Cairo, Egypt.

*Polycrystalline powder of nanostructural ZnSe was successfully prepared by Inert Gas Condensation (IGC) method. The Energy Dispersion Analysis of X-ray (EDAX) showed that the ZnSe films have the atomic ratio of Zn:Se = 1:1.25. The structure characteristics of the prepared samples were investigated by X-Ray Diffraction (XRD) technique. Materials deposited at temperatures less than -30 °C show amorphous structure. Also, the as-deposited (-30 °C) and annealed (80 °C, 60 min) films of 110 nm thick have not ensured their crystallinity. However, the results of the collected powder that scraped from the films confirmed the presence of crystalline nanostructural ZnSe of cubic zinc blende structure with lattice parameter  $a_0 = 0.5670$  nm. The grain size and size distribution of the powder sample was determined by line profile analysis using WinFit computer program and Fourier analysis. It was found that crystallite size is  $\approx 3.6$  nm. The size distribution characterized by being asymmetrical unimodal and skewed towards small size with maximum fraction at crystallite size of  $\approx 1.2$  nm. On the other hand, the cumulative size distribution shows that 50% volume fraction exhibits crystallites finer than 2.3nm.*

## 1. Introduction:

Nanocrystalline materials exhibit an atomic structure which differs from that of the two known solid states: the crystalline (long-range order) and amorphous (short-range order) [1]. They are polycrystals; the crystallite size of which is a few nanometers (1-10 nm). Materials of grains in the order of 100 nm in diameter are also considered as nanomaterials [2]. Research on nanocrystalline solids was initiated about two decades ago [3]. When the grain size is about a few lattice constants, the volume fraction of boundary cores (incoherent interface between crystallites) approaches 50% or more of the solid. In this case, the structure as well as the properties of such solid are

controlled by the structure and properties of the grain boundary core regions. Such materials are characterized not only by the grain size but also by their size distribution. The properties of nanocrystalline materials differ (in some cases by several order of magnitude) from those of glasses and/or crystals with the same chemical composition [1]. Therefore, they open the way for generating solid materials with new and interesting properties, which suggests that they may be utilized technologically in the future.

Nanoparticles and nanostructural materials represent an evolving technology that has an impact on an incredibly wide number of industry and markets. Recently, much interest has been focused on semiconductor nanocrystals because they exhibit strongly size-dependent optical and electrical properties. These characteristics open new applications including high performance optoelectronic devices [4]. The manufacture of nanoparticles can be achieved through a number of different techniques including colloidal methods, rf sputtering, molecular-beam epitaxy [4], pulsed laser deposition [5] and inert gas condensation (IGC) [6]. ZnSe is an important material for research due to its interested optical behaviour [7 & 8] and its potential in many industrial applications as photovoltaic window [9-11] and laser diodes [12 & 13].

The aim of this work is, first, to prepare nanocrystalline materials of ZnSe semiconductor using the IGC technique. Second, the structural characteristics (phase identification, crystallite size and size distribution) of the prepared materials will be also studied by X-ray diffraction (XRD) line profile analysis.

## **2. Experimental:**

The samples were prepared by IGC technique [6] using ZnSe ingot powder (as received) of purity 99.999 %. They were deposited using cold finger configuration and thermal evaporator. The deposition was accomplished on cooled clean glass substrates at low pressures of 15-20 Pa of argon gas. The prepared films were deposited perpendicular to the substrate surface. The deposition temperature was measured with temperature controller and thermocouple attached to the substrate. Preparation was carried out at substrate temperature ranging from -95°C to -10°C. A film thickness monitor (Edwards FTM5, England) was used to control the film deposition rate and to estimate the film thickness. The thickness of the prepared films was about 110 nm. The powder sample was collected by scraping the deposited films from the glass substrate.

The atomic composition of the deposited films is realized by the elemental analysis using Energy Dispersive Analysis of X-ray (EDAX) technique (Philips, XL30). Computer controlled X-ray diffractometer (Diano-8000, USA) with monochromatic Co- $K_{\alpha}$  radiation was used for structural investigation and grain size determination of the prepared samples. The scanning range was  $10-75^{\circ}$  ( $2\theta$ ) with step size of  $0.02^{\circ}$  ( $2\theta$ ) and counting time of 5 second per step. Data analysis was accomplished by the WinFit computer program of Krumm [14].

### 3. Results and discussion:

#### 3.1. Phase Characterization:

The X-ray diffraction pattern of the as received ingot ZnSe powder is shown in Fig. (1). It shows that the ingot powder is polycrystalline and phase identification indicates the presence of the cubic zinc blende structure (ICCD # 80-0021 X-ray file). The principal diffraction peaks and the Miller indices for the used ZnSe powder are depicted.

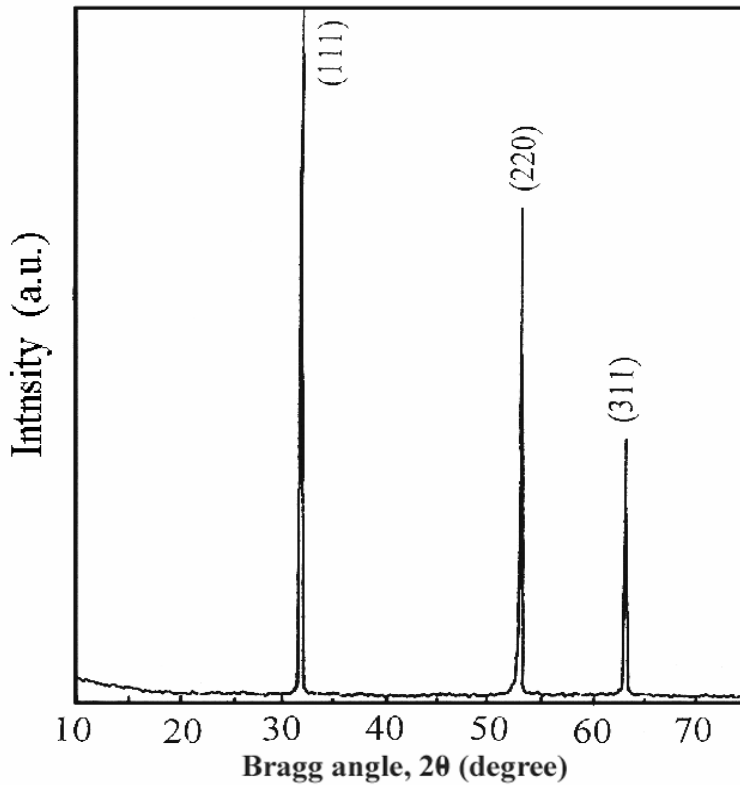


Fig.(1): X-ray diffractogram of the as received ingot ZnSe powder.

The energy dispersive analysis of X-ray (EDAX) of ZnSe films deposited at  $-30^{\circ}\text{C}$  is depicted in Fig. (2) and the results are given in Table (1). A slight deviation from stiochiometry was observed where the atomic ratio of Zn:Se  $\approx 1:1.25$ .

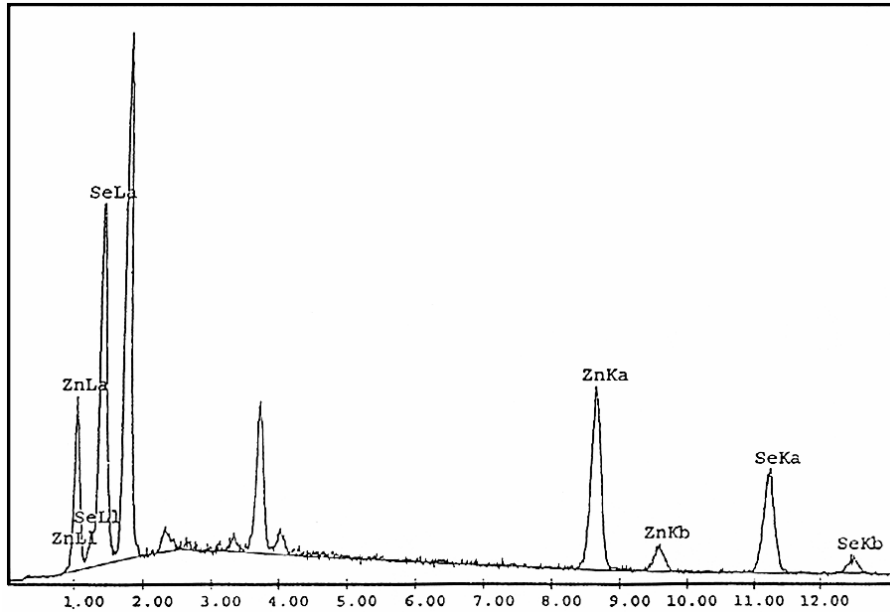


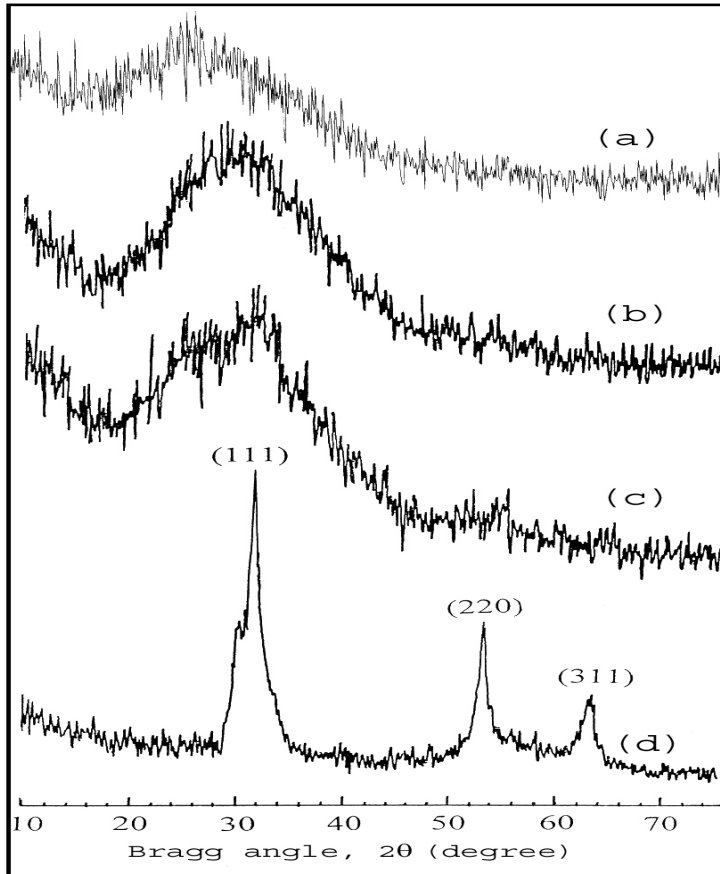
Fig.(2): The energy dispersive analysis of X-ray (EDAX) for ZnSe nanocrystallite Film.

Table (1): Elemental analysis (EDAX data) of as-deposited ZnSe thin film.

Element	Wt %	At %
Zn	39.78	44.38
Se	60.22	55.62
Total	100.00	100.00

Films deposited at temperature in the range from  $-10^{\circ}\text{C}$  to  $-95^{\circ}\text{C}$  and the corresponding scraped powder were studied by XRD techniques to show the effect of the deposition temperature on the crystallinity of the material. Those deposited at temperatures less than  $-30^{\circ}\text{C}$  showed amorphous structure. Figure (3) shows the diffractograms of the glass substrate, the as-deposited film at  $-30^{\circ}\text{C}$  as well as that annealed at  $80^{\circ}\text{C}$  for 60 min and the scraped ZnSe powder. Comparison with the diffractogram of the substrate (Fig. 3a) and the observed change in the diffractogram of the annealed films as well as the relatively large film thickness ( $=110\text{ nm}$ ) verify that the observed hump is not

related to that of glass. However, the XRD patterns of films, Figs.(3 b & c), could not verify the crystalline nature of the films even after annealing at 80 °C for 60 min. This may be predominantly due to the small size of the grains and also the small amount of material that exposed to X-ray in case of films compared to the powder form. Thus, respectively, large broadening and low intensity of the diffraction peaks are expected. On the other hand, the three peaks corresponds to (111), (220) and (311) planes of ZnSe of zinc blend structure were marked in Fig. (3 d) of the powder sample that collected by scraping from the films.



**Fig.(3):** X-ray diffractograms of: a) glass substrate, b) as-deposited ZnSe film, c) film annealed at 80°C for 60 min. and d) collected powder.

The calculated lattice parameter,  $a_0$ , from the (220) reflection equals 0.5670 nm. It is slightly larger than 0.5618 nm of that given in ICCD # 80-0021 and in agreement with 0.5668 nm of that given in ICCD # 37-1463. According

to the EDAX results (higher Se ratio than the stoichiometry), this seems to be due to the larger ionic radius of  $\text{Se}^{2-}$  ( $= 0.198 \text{ nm}$ ) relative to  $\text{Zn}^{+2}$  ( $= 0.074 \text{ nm}$ ). Also, the presence of interstitial lattice defects is possible.

### 3.2. Profile Analysis:

Exact profile of a reflection has to be known for determination of crystallite size and lattice strain, specially if Fourier analysis is used. Any smoothing procedure may lead to distortion of the original peak profile and may introduce significant errors into the data [15]. A better way is to model an analytical profile shape function (PSF) to the experimental data in order to calculate the peak parameters. Accordingly, WinFit program [14] is going first to fit PSF and to use the refined profile parameters for the determination of crystallite size and internal residual strain by one-order (single line) method or multi-order procedure. In this work, the split Pearson VII function (mixing of Gaussian and Lorentzian shape) was used as the PSF. The observed data ( $I_{\text{obs}}$ ), the calculated fitted reflection ( $I_{\text{calc}}$ ) and difference pattern are presented in Fig.(4). The numerical criteria of fit is the discrepancy,

$$R = \frac{\sum (I_{\text{obs}} - I_{\text{calc}})^2}{\sum (I_{\text{obs}})^2}.$$

In WinFit program,  $(1-R) \%$  is given as a measure for the reliability. An accepted value of 94.38 % is obtained.

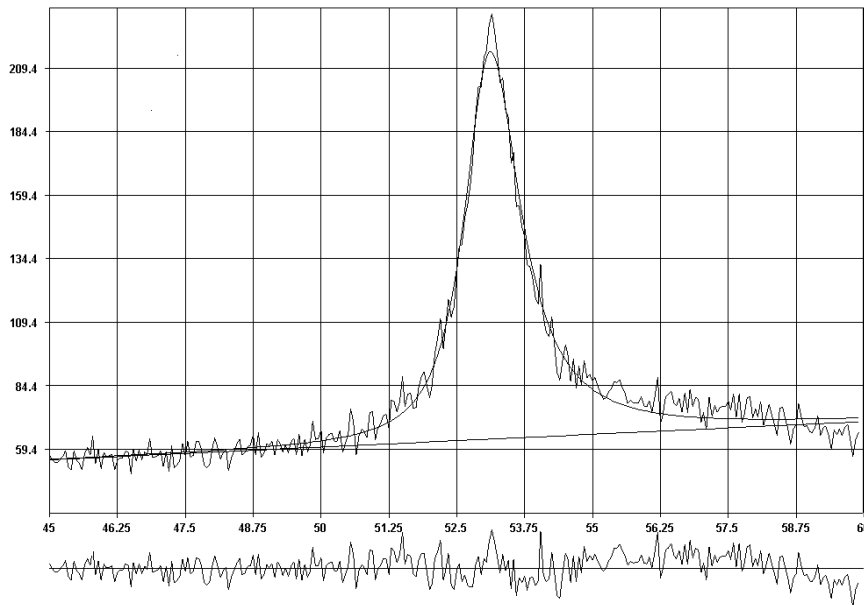


**Fig.(4):** Fitting of (220) diffraction line of the prepared powder sample (The observed and the calculated intensities, and the difference).

**A) Crystallite Size:**

In this work, the main interest is the crystallite size and size distribution of the deposited powder and they were calculated by Fourier analysis using single line approach. The crystallite size was estimated from the (220) diffraction line at  $2\theta \approx 53.036^\circ$  and the annealed ingot sample was used as the standard one. Figure (5) shows the diffraction line of the sample and that of the standard.

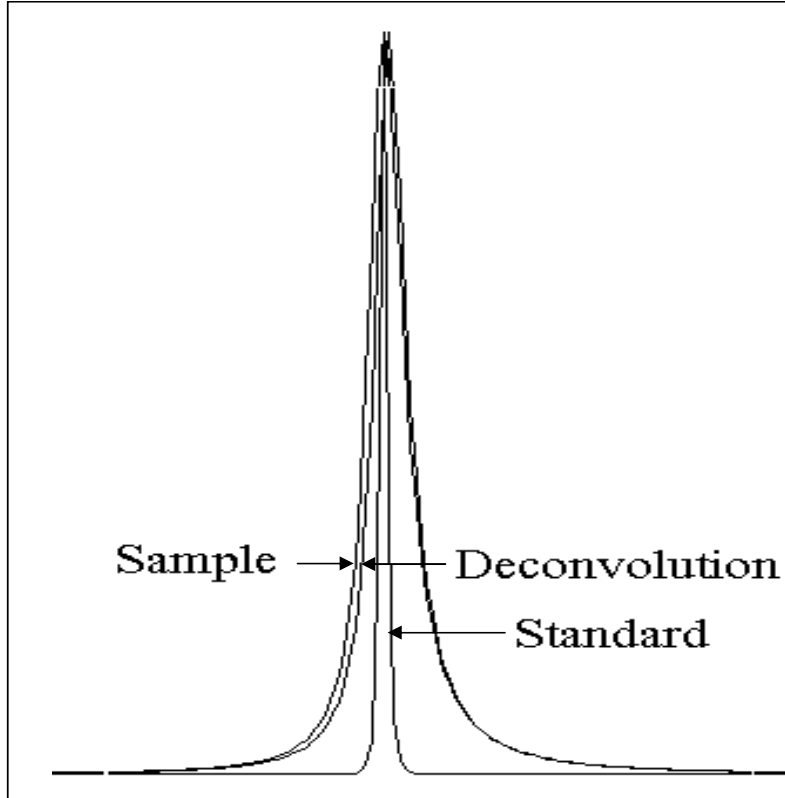


**Fig.(5):** The (220) diffraction line of the prepared powder sample and that of the standard as well as the corrected (deconvoluted) profile.

The size parameters are calculated by Fourier analysis. The instrumental dependent broadening was removed by deconvolution Fourier-method of Stokes [16] using a modified routine [17]. The corrected profile is Fourier transformed according to Warren-Averbach analysis [18 & 19]. The Fourier coefficients  $F(L)$  are plotted versus a distance, the domain size  $L = na_3$ , normal to the reflecting plane, where  $n$  is the harmonic number and  $a_3$  is a length depending on the  $d$ -spacing of the reflecting plane (direct proportional)

and the period length of the Fourier series (inverse proportional). The steepest part is linearly extrapolated to  $F(0)$  and all values are normalized ( $A(L) = F(L)/F(0)$ ) to give  $A(0) = 1$ . The plot of Fourier coefficient  $A(L)$  versus the domain size  $L$  is shown in Fig. (6). The linear extrapolation towards  $A(L) = 0$  yields the mean coherently diffraction domain or the area weighted average crystallite size. From the intercept of the straight part with the x-axis an average value of the crystallite size was estimated as 3.6 nm.

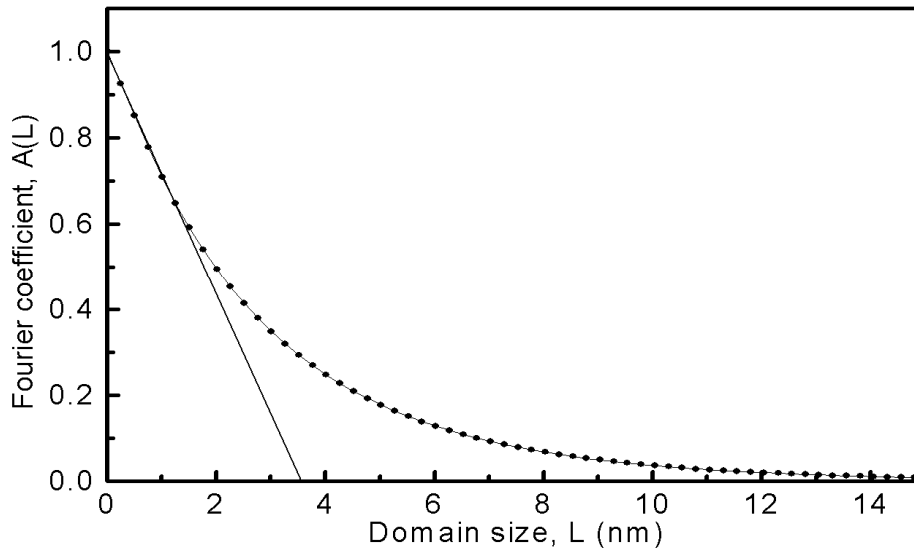


Fig.(6): Plot of normalized Fourier coefficient  $A(L)$  versus domain size  $L$ .

### B) Size Distribution:

In real mass of powder, although all the grains are prepared in the same manner, they will not have the same exact size, even though the shape may be the same. Consequently, one must deal with size distribution when accurately describing powders. An average value of a single dimension may be inaccurate for certain shapes. Even for equiaxed grains such an average value may be misleading. Therefore, the distribution curves that relate the grain size to the corresponding fraction of the powder with that size are required.

The second derivative of Fourier coefficients  $A(L)$  with the domain size  $L$  ( $d^2A(L)/dL^2$ ) gives this distribution, Fig. (7). It is clear that the distribution curve is asymmetrical unimodal and skewed towards small size with crystallite size of  $\approx 1.2$  nm corresponding to the maximum fraction. Cumulative size curve can be also presented. Either the volume fraction per cent less than or greater



than a specific size value is plotted as a function of the size. In Fig. (7) the cumulative grain size distribution for the first case (% finer) is illustrated. The crystallite size corresponding to 50% volume fraction is  $\approx 2.3$  nm.

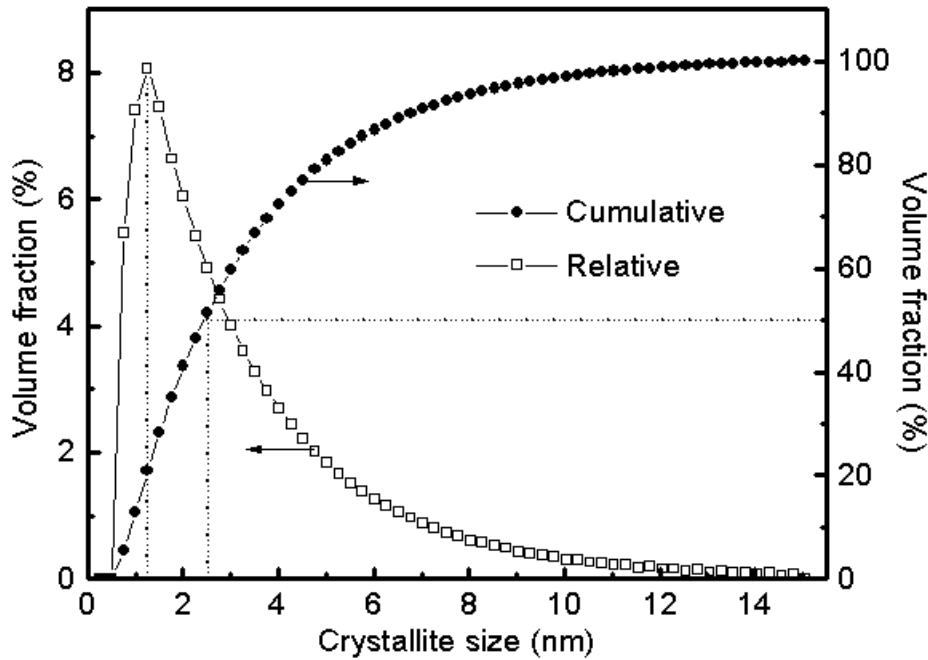


Fig.(7): Relative and cumulated crystallite size distributions.

### Conclusion:

Nanocrystalline ZnSe powder can successfully be deposited by IGC method in a temperature range of  $-10$  to  $-30$  °C and Argon pressure of  $\approx 15 - 20$  Pa. Deposition at temperatures less than  $-30$  °C results in amorphous materials. The phase of the prepared powder is ZnSe with cubic system of zinc blende structure and lattice parameter  $a_0 = 0.5670$  nm. The estimation of the crystallite size shows different values from different approaches (curves) but all verify the nanocrystalline nature of the prepared powder. The crystallite size is  $\approx 3.6$  nm,  $2.3$  nm and  $1.2$  nm as defined from Fourier analysis, cumulative distribution and relative distribution, respectively. The size distribution characterizes by being asymmetrical unimodal and skewed towards small size.

**References:**

1. H. Gleiter, *J. Appl. Cryst.*, **24**, 79 (1991).
2. W. Xiao-Dong, M. G. Jiang-Norton and K. W. Hipps, *Thin Solid Films*, **251**, 121 (1994).
3. P. Marquardt and H. Gleiter, *Verh. Dtsch. Phys. Ges.*, **15**, 328 (1980).
4. L. E. Brus, A. Efros and T. Itoh, *J. Lumin.*, **76**, 1 (1996).
5. Xu NingBoo and Bong Hyun, *Semi. Sci. and Tech.*, **18**, 300 (2003).
6. R. Birringer, H. Gleiter, H. P. Klein and P. Marquardt, *Phys. Lett.*, **102A**, 365 (1984).
7. Hyun-Yong Lee, Seon-Ju Kim, Jin-Woo Kim and Hong-Bay Chung, *Thin Solid Films*, **441**, 214 (2003).
8. P. Reiss, G. Quemard, S. Carayon, J. Bleuse, F. Chandezon and A. Pron, *Mat. Chem. And Phys.*, **84(1)**, 10 (2004).
9. J. Herrero, M. T. Gutierrez, C. Guillen, J. M. Dona, M. A. Martnez, A. M. Chaparro and R. Bayon, *Thin Solid Films*, **361-362**, 28 (2000).
10. C. Calderon, H. Infante and G. Gordillo, *Surface Rev. and Lett.*, **9**, 1617 (2002).
11. G. Gordillo, *Surface Rev. and Lett.*, **9**, 1675 (2002).
12. K. Ohkawa, T. Karasawa and T. Mitsuyu, *Japan J. Appl. Phys.*, **30**, L152 (1992).
13. J. M. Gaines, R. R. Drenten, K. W. Haberern, T. Marshall, P. Mensz and J. Petruzzello, *Appl. Phys. Lett.*, **62**, 2462 (1993).
14. S. Krumn; XIII th Conference on Clay Mineralogy and Petrology, Praha (1994), *Acta Universitatis Carolinae Geologica*, **38**, 253 (1994).
15. S. A. Howard and K. D. Preston, "Modern Powder Diffraction", Edt. by D. L. Bish and J. E. Post, *Reviews in Mineralogy*, **20**, 217 (1989).
16. A. R. Stokes, *Proc. Phy. Soc. (London)*, **61**, 382 (1948).
17. W. H. Press, S. A. Teukolsky, W. T. Vetterling and B. P. Flannery, "Numerical Recipes in C – the Art of Scientific Computing", Second edition, Cambridge Univ. Press, p. 994 (1992).
18. B. E. Warren, *Progress in Metal Physics*, **8**, 147 (1959).
19. H. Natter, M. Schmelzer, S. JanBen and R. Hempelmann, *Ber. Bunsenges. Phys. Chem.*, **101**, 1706 (1997).